Electrical Behaviour of Twist Grain Boundary Phases of 4-*n*-dodecyloxy-4'-(cholesteryloxycarbonyl-1-butyloxy) chalcone

Abhay S. Pandey[1,*], R. Dhar[1], A. S. Achalkumar[2] and C. V. Yelamaggad[2]

[1]*Soft Materials Research Laboratory, Centre of Material Sciences, Institute of Interdisciplinary Studies, Nehru Science Complex, University of Allahabad, Allahabad -211002, India*

[2]*Centre for Soft Matter Research, P. B. No. 1329, Prof. U. R. Rao Road, Jalahalli, Bangalore -560013, India*

Abstract: There are only few compounds, which have shown wide temperature range twist grain boundary (TGB) phases. One such compound is the cholesterol derived, 4-*n*-dodecyloxy-4'-(cholesteryloxycarbonyl-1-butyloxy) chalcone, which shows a wide temperature range TGBA (~ 11 °C) and TGBC* (~ 19 °C). In the present work, we are reporting the temperature and frequency dependence of the dielectric parameters of the above compound for two different conditions of molecular anchoring i.e. planar and homeotropic. The dielectric studies have been carried out in the frequency range of 1 Hz to 35 MHz. In homeotropically aligned sample, the experimental dielectric spectra display a feeble relaxation mode in TGBA and TGBC* phases in MHz frequency range. Planar oriented molecules show a soft mode like relaxation due to the tilt fluctuation of molecules in MHz region for both the TGB phases and support theoretical formulation for the soft mode relaxation of the TGB phases. Various dielectric parameters have been determined for the two TGB phases of the above mentioned compound.

Keywords: Chiral liquid crystals, Liquid crystal dimers, TGB phases, Dielectric relaxation spectroscopy, Dielectric strength slopes, Rotational viscosity.

1. INTRODUCTION

Chirality in functional molecular materials is a powerful tool for inducing properties and molecular organizations absent in nonchiral materials. This is particularly true in mesogenic materials. For instance, the twist-grain boundary (TGB) phase is a type of frustrated phases with absorbing physical and structural features, which are found exclusively in optically active systems. TGB phases have been known since 1988 [1] and have attracted great consideration during the last two decades. Chiral liquid crystals have the tendency to form a cholesteric-like helical director field. On the other hand, the molecular interactions may favor a smectic layer structure. However, it is impossible to realize a continuous structure which exhibits both a cholesteric director field and a smectic layer structure at the same time. The competition between these two structural features can result in frustrated structures containing a regular lattice of grain boundaries, which in turn consist of a lattice of screw dislocations. This defect structure exhibits an interesting theoretical analogy to the flux line lattice which occurs in the Shubnikov phase of type II superconductors. However, the range of parameters determining the structure is larger in liquid crystals than in superconductors. A large variety of new phases, such as the TGBA [1], TGBC [2], TGBC* [3], melted grain boundary [4] phases, a defect line liquid (N^*_L) [5], antiferroelectric crystals of twist grain boundaries [6], and smectic blue phases [7] have been predicted and/or experimentally observed. The first experimental observation of TGBA phase was reported by Goodby *et al.*, [8, 9]. As shown in Fig. (**1a**), a TGBA phase consists of smectic slabs, separated by defect walls (grain boundaries) consisting of defect lines (twist dislocations). In the slabs, molecules are arranged in layers with their director normal to the smectic layers. Neighboring slabs (and hence molecular director in the slabs) are twisted with respect to each other by an angle $\Delta\chi$, thereby forming a helical structure with the helix axis normal to the molecular director [1, 10, 11]. The length along the helical axis corresponding to the twist of smectic slabs (l_b), distance between defect lines (l_d) and pitch (P) are related by equation:

$$\alpha = \frac{\Delta\chi}{2\pi} = \frac{l_b}{P} = \frac{1}{\pi}\tan^{-1}\left(\frac{d}{2l_d}\right) \approx \frac{1}{\pi}\sin^{-1}\left(\frac{d}{2l_d}\right)$$

where d is the layer spacing and α, a number. If α is irrational, the structure is incommensurate, i.e. there is no periodicity of the orientation of the slabs along the pitch axis; however, if α is rational, the system is commensurate and has an n-fold screw axis.

Two more TGB phases, namely TGBC and TGBC* were predicted by Renn and Lubensky [2, 3]. The schematic demonstration for TGBC* phase are shown in Fig. (**1b**). These would correspond to Abrikosov vortex lattices in a hypothetical superconductor wherein Ginzburg parameter (k) is negative and there is Bose condensation. Renn [3] derived the mean-field phase diagram of N*-SmA-SmC* within the framework of the chiral Chen-Lubensky model, which

*Address correspondence to this author at the Soft Materials Research Laboratory, Centre of Material Sciences, Institute of Interdisciplinary Studies, Nehru Science Complex, University of Allahabad, Allahabad-211002, India; Tel: +919839108905; Fax: +915322460017;
E-mail: abhaypandey.liquidcrystal@gmail.com

1874-8465/11 2011 Bentham Open

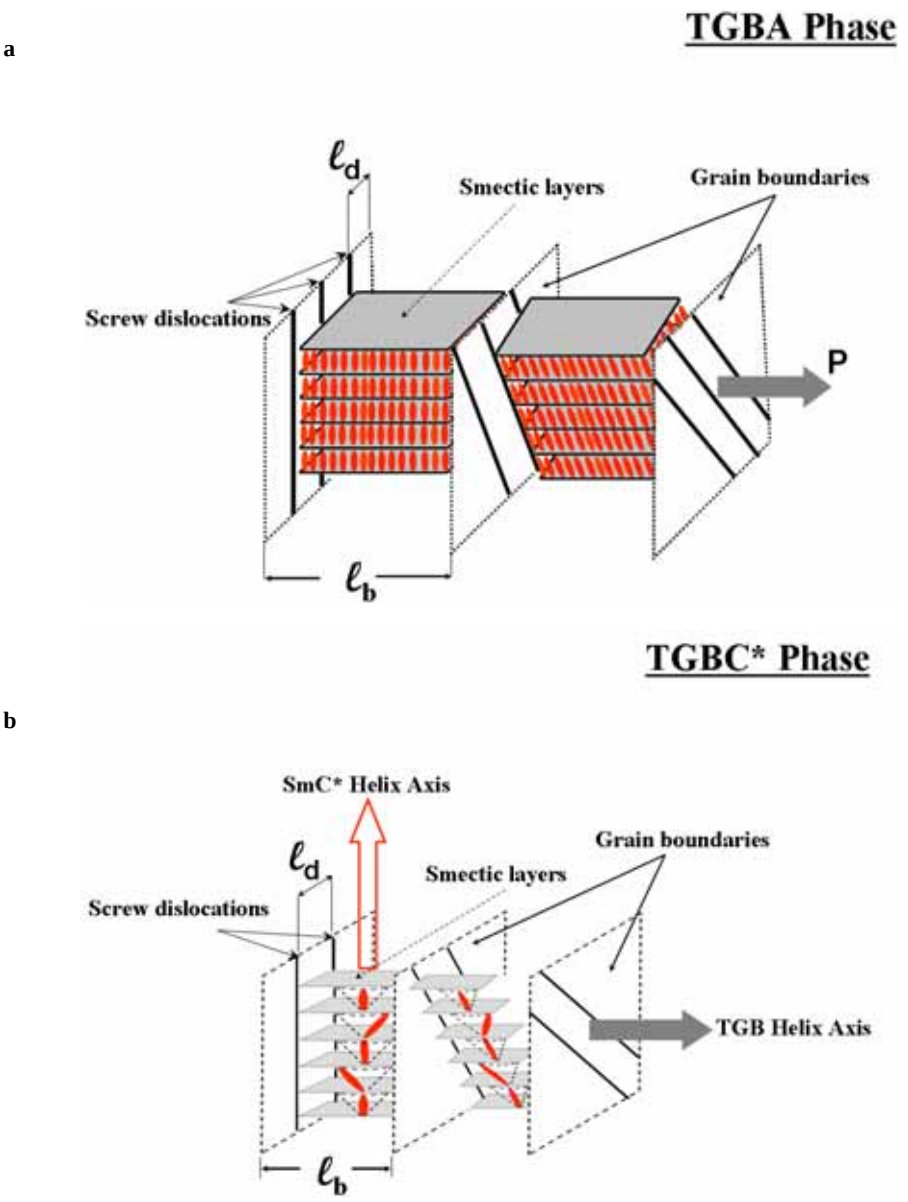

Fig. (1). Schematic representation For (**a**) TGBA and (**b**) TGBC* phase.

showed the existence of TGBC and TGBC* phases. He showed that the TGBA-TGBC transition is replaced by TGBA-TGBC* transition when the cholesteric pitch length P increases beyond ~$2P_C$ /3, where P_C is the pitch length of SmC*. In the proposed TGBC structure [3], directors of the molecules in the smectic slabs are tilted with respect to the smectic layer normal. In TGBC* phase, slabs are filled by SmC* structure and thus TGBC* has two helices that are mutually perpendicular to each other. N^*_L phase is the analog of the flux line liquid occurring in type II superconductors with strong fluctuations expected between N^* and TGBA phases [5] and it has been experimentally observed in some materials [12, 13]. Present study reports the temperature and frequency dependence of the dielectric properties of the cholesterol derived optically active unsymmetrical liquid crystalline dimeric compound 4-*n*-dodecyloxy-4'-(cholesteryloxycarbonyl-1-butyloxy) chalcone. Synthesis and preliminary characterization of different phases of the material is previously reported [14].

2. EXPERIMENTAL

Using polarized light microscopy the different phases in the compound have been identified in the earlier published work [14], and re-confirmed in this study as well. The dielectric measurements for the planar aligned sample were carried out with a dielectric cell in the form of parallel-plate capacitor from AWAT, Warsaw. Electrodes of the cell are gold coated glass plates and separated by spacer of thickness 8.8 μm. Active capacitance (C_A) of cell was 34.0 pF. For the homeotropic alignment, the dielectric cell in the form of parallel-plate capacitor was prepared using gold-coated glass plates, having a sheet resistance of less than 1.0-1.5 Ω and chemically treated with lecithin. The material has been filled in the cell in its isotropic liquid phase at a temperature above 10 ℃ to clearing point. Dielectric data have been acquired by using the Newton's Phase Sensitive Multimeter (model-1735) coupled with Impedance Analysis Interface (IAI model-1257), in the frequency range of 1 Hz to 35 MHz. The

temperature of the sample was controlled with the help of a hot stage (Instec model HS-1) having an accuracy of ± 0.1 °C and a resolution of 3 mK. The temperature near the sample has been determined by measuring thermo-emf of a copper-constantan thermocouple with the help of a six and half digit multimeter from Agilent (model-34410A) with the accuracy of ± 0.1 °C. The active capacitance (C_A) of the homeotropic cell has been determined by using standard non-polar liquid (cyclohexane in this case) as follows:

$$C_A = [C(ch) - C(a)]/[\varepsilon'(ch) - 1], \quad (1)$$

where C(ch) and C(a) are the capacitance of the cell filled with cyclohexane and air respectively, ε'(ch) is the relative permittivity of cyclohexane. Complete removal of the cyclohexane (after the calibration) from the cell was ensured by comparing the capacity of the cell before and after filling the cyclohexane. The dielectric permittivity and loss of the material have been calculated with the help of the following equations:

For homeotropic cell

$$\varepsilon' = [\{C(m) - C(a)\}/C_A] + 1 \quad (2a)$$

For planar aligned cell

$$\varepsilon' = C(m) / (C_A = 34.0\ pF) \quad (2b)$$

and

$$\varepsilon'' = 1/2\,\pi\, f\, RC_A \quad (3)$$

where å' and å'' are the dielectric permittivity and loss, respectively; C (m) is the capacitance of the cell filled with material; f the frequency; and R the resistance of the material filled between parallel glass plates.

In the case of dispersive material, the measured dielectric spectrum can be described with the help of generalized Cole-Cole equation [15, 16]:

$$\varepsilon^* = \varepsilon' - j\varepsilon'' = \varepsilon(\infty) + \sum_i \frac{(\Delta\varepsilon)_i}{1 + (j f\ \tau_i)^{(1-h_i)}} + \frac{A}{f^n} - j\frac{\sigma_{ion}}{2\pi\varepsilon_0 f^k} - jBf^m \quad (4)$$

where $(\Delta\varepsilon)_i$, τ_i and h_i are the dielectric strength, the relaxation time (inverse of relaxation frequency) and the symmetric distribution parameter ($0 \le h_i \le 1$) of the i^{th} mode, respectively; ε(0) and ε(∞), the low and high frequency limiting values of the relative dielectric permittivity; and the third and fourth terms in Equation (4), represent the contribution of the electrode polarization capacitance and ionic conductance at low frequencies where A and n are constants [17]. In the case of pure ohmic conductance, constant k is found to be 1. The fifth imaginary term Bf^m is included in Equation (4) to partially account for the high-frequency electrode surface resistance [18, 19], B and m being constants as long as correction is small and ε_0 (=8.85 pFm^{-1}) is the free space permittivity. Real and imaginary part of Equation (4) can be written as follows:

$$\varepsilon' = \varepsilon(\infty) + \sum_i \frac{\Delta\varepsilon_i[1 + (\omega\ \tau_i)^{(1-h_i)}\sin(h_i\pi/2)]}{1 + (\omega\ \tau_i)^{2(1-h_i)} + 2(\omega\ \tau_i)^{(1-h_i)}\sin(h_i\pi/2)} + \frac{A}{f^n} \quad (5)$$

and

$$\varepsilon'' = \sum_i \frac{\Delta\varepsilon_i(\omega\ \tau_i)^{(1-h_i)}\cos(h_i\pi/2)}{1 + (\omega\ \tau_i)^{2(1-h_i)} + 2(\omega\ \tau_i)^{(1-h_i)}\sin(h_i\pi/2)} + \frac{\sigma_{ion}}{2\pi\varepsilon_0 f^k} + Bf^m \quad (6)$$

To explore the expected mode of relaxation in these systems, the dielectric permittivity and loss data have been fitted with the help of Equations (5) and (6). We have subtracted low frequency correction terms due to electrode polarization capacitance from the measured data to explore relaxation phenomenon in TGBA and TGBC* phases.

3. RESULTS AND DISCUSSION

The chemical structure of the investigated compound is shown in Fig. (**2**). Optical texture study under the polarizing light microscope is a fundamental tool for classifying liquid-crystalline phases. TGB phases are also most often characterized on the basis of their characteristic textures under different types of anchoring of molecular directors. A very characteristic pattern for a TGBA phase is the filament texture shown in Fig. (**3a**), which occurs for the anchoring of the director normal to the bounding surfaces of the sample (homeotropic). The TGBC* phase also shows the filamentary textures in homeotropic alignment as shown in Fig. (**3b**). The filaments observed in the TGBC* phase are different from the TGBA phase. The TGBC* filaments are undulatory in nature, the period of undulation being about the same as that of the square grid pattern obtained in the planar geometry [20]. The phase sequence of investigated compound as obtained from the polarized light microscopy and differential scanning calorimetry are given below,

In the Heating Cycle

Crystal 114.3 °C (49.4) TGBA 124.9 °C (8.7) Isotropic liquid;

In the Cooling Cycle

Isotropic liquid 121.2 °C (8.3) TGBA 106.7 °C (0.2) TGBC* 74.2 °C (28.2) Crystal.

Where data in parentheses are enthalpies (Jg^{-1}), whereas those outside the parenthesis are transition temperature (°C) associated with phase transitions.

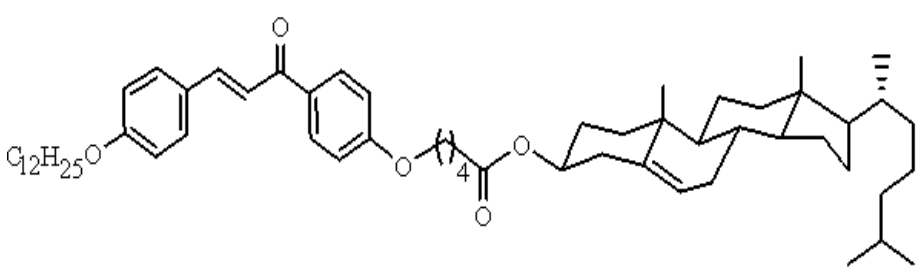

Fig. (2). Molecular structure of optically active dimeric compound, 4-*n*-dodecyloxy-4'-(cholesteryloxycarbonyl-1-butyloxy) chalcone.

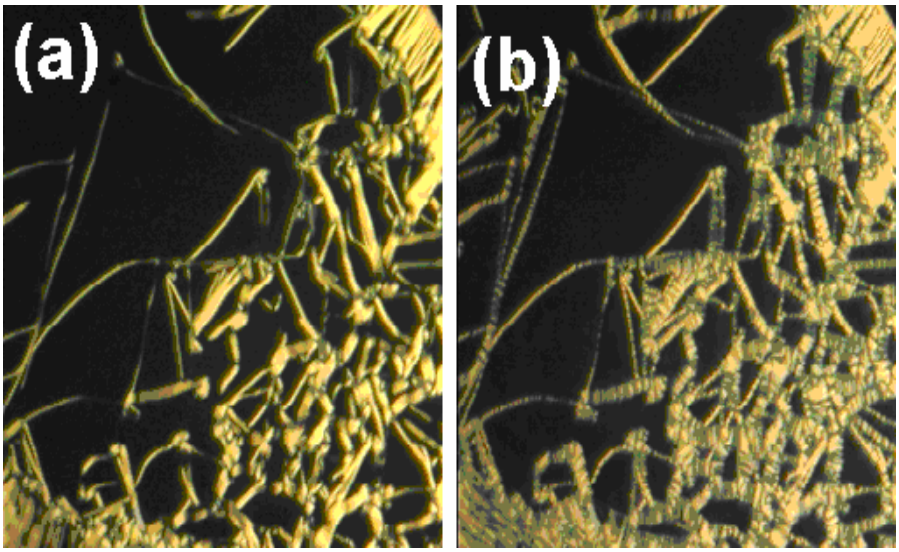

Fig. (3). Optical textures observed for 4-*n*-dodecyloxy-4'-(cholesteryloxycarbonyl-1-butyloxy) chalcone on slides treated for homeotropic orientation: (**a**) filaments of TGBA growing from the isotropic liquid phase; (**b**) undulated filaments of TGBC* phase.

Dielectric studies have been carried out in planar and homeotropic configurations in the frequency range of 1 Hz to 10 MHz of the compound 4-*n*-dodecyloxy-4'-(cholesteryloxycarbonyl-1-butyloxy) chalcone for which TGB phase have been observed. It has been examined that dielectric permittivity in planar configuration ($\varepsilon_{\perp}^{'}$) in the isotropic liquid phase is almost constant with the frequency in the frequency range 1 Hz to 35 MHz, implying that no dipolar relaxation phenomenon occurs in this frequency range. However, in the TGBA and TGBC* phases, permittivity value shows dispersion with the frequency. This is because of the presence of a feeble dielectric relaxation mechanism in the MHz frequency region as shown in Fig. (**4a**) for TGBC* phase. Similar mechanism has been observed for the TGBA phase. But observed strength in TGBA phase is weaker than the TGBC* phase. The dielectric permittivity and loss fitted data for TGBC* phase at 93.2 ℃ is given in Figs. (**4a**) and (**4b**) respectively. The relaxation phenomenon for TGBC* phase in the Cole-Cole plot at 93.2 ℃ is shown in Fig. (**5**). The dielectric strength and relaxation frequency of the observed mode has been found to be in the ranges of ~1.0-1.4 and ~3.7-7.9 MHz respectively for these phases as shown in Fig. (**6**). The magnitude of the dielectric strength observed in this work is almost the same as observed by Ismaili *et al*., [21], but relaxation frequencies are marginally towards higher side. Difference of the relaxation frequencies may be featured to different shape and size of the molecules in the above two cases. Molecular interactions depend upon the functional group attached with the molecules which are also different in two different studies and may be the cause of difference in the relaxation frequencies. In the research of Ismaili *et al*., [21], molecular interactions seem larger (due to the presence of fluorine) than in this system. It may be useful to remind here that the soft mode is due to the amplitude fluctuation of group of molecules. Strong molecular interaction produces a large group of molecules which will cause low soft mode relaxation frequency as observed in the research of Ismaili *et al*., [21]. It is important to mention that the variations of both the dielectric strength and relaxation frequency are continuous at TGBA-TGBC* transition. There is no drastic change at the transition as it usually happens in the case of soft mode (of the SmA* phase) to Goldstone mode (of the SmC* phase) transitions in the ferroelectric liquid crystalline materials. Hence, on the basis of the magnitude and temperature dependence of the dielectric strength and relaxation frequencies, we presume the mode as soft mode of the TGBA and TGBC* phases. It is important to talk about the strength of the observed soft mode is $(\Delta\varepsilon_{\perp})_{SM} = \varepsilon(0) - \varepsilon'(\infty)$, where $\varepsilon(0)$ is the low frequency limiting value of dielectric permittivity and $\varepsilon'(\infty)$ is the lowest value of dielectric permittivity corresponding to the soft mode. It is expected that another relaxation mode corresponding to the rotation of molecules about their short axes will exist above 10 MHz and strength of this mode would be $\varepsilon'(\infty)$-$\varepsilon(\infty)$. Taking crystal phase dielectric permittivity data (~2.6) approximately as $\varepsilon(\infty)$, strength of the relaxation mode corresponding to the rotation of molecules about their short axes is expected to be ~0.6.

In the homeotropic anchoring of molecules, it has been observed that the dielectric permittivity in the isotropic liquid phase is almost constant with the frequency in the frequency range 1 Hz to 10 MHz as observed in planar configuration, implying that no dipolar relaxation phenomenon occurs in this frequency range. However, in the TGBA and TGBC* phases, a relaxation mechanism occurs on higher frequency region side. The Cole-Cole fitting of dielectric permittivity and dielectric loss for TGBC* phase is given in Figs (**7a**) and (**7b**) respectively. In Fig. (**8a**), the relaxation mode (in inset) and the relaxation peak of the cell are shown, a three dimensional plot given in Fig. (**8b**), which shows this mode at different temperatures. The dielectric strength and relaxation frequency of the observed mode has been found to be in the ranges of ~0.4-0.7 and ~3.2-5.4 MHz respectively for TGBA and TGBC* phases. The nature of the molecular

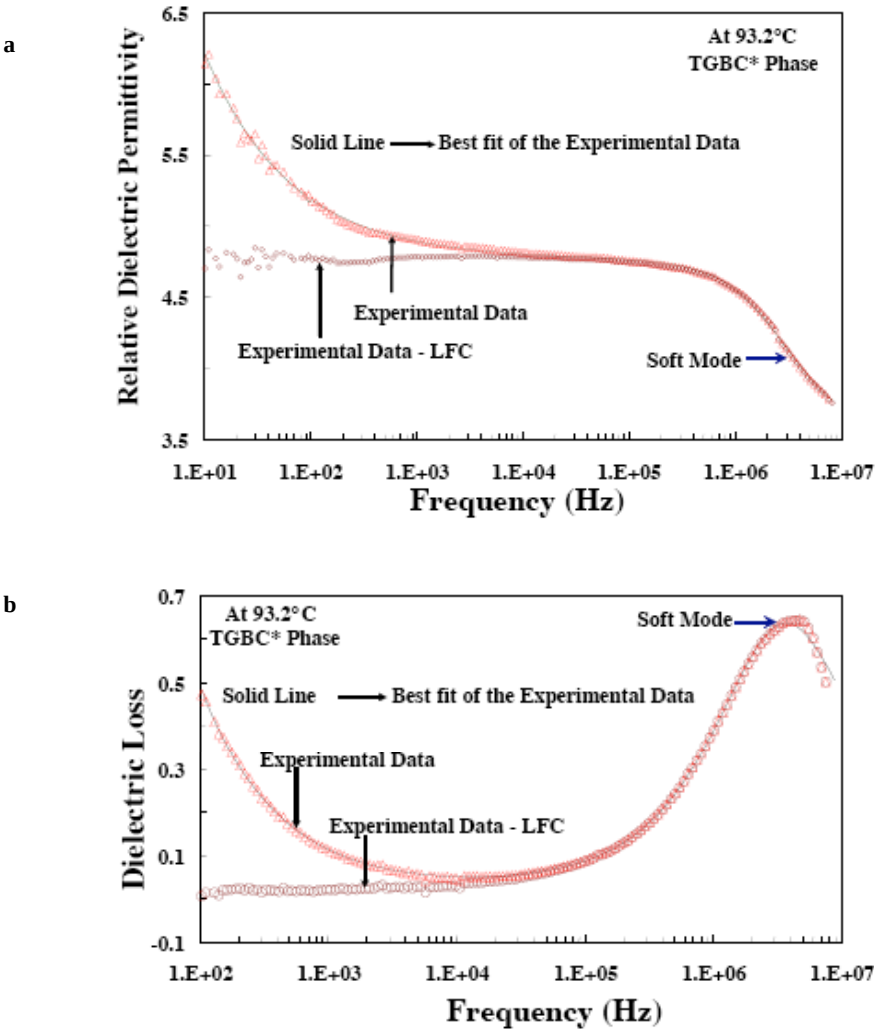

Fig. (4). Frequency dispersion of (**a**) dielectric-permittivity and (**b**) dielectric loss at 93.2 ℃ in the TGBC* phase for the planar anchoring of the molecules to demonstrate signatures of the soft mode (on the higher frequency side). The solid line is fit of Cole-Cole formula.

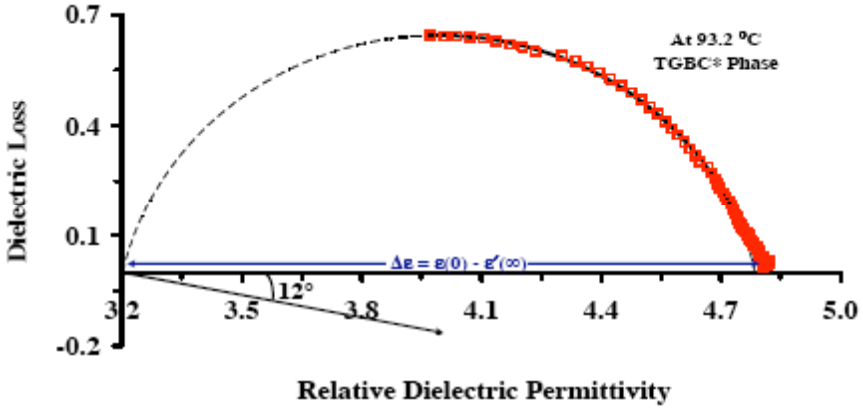

Fig. (5). Cole-Cole plot for the soft mode of TGBC* phase at 93.2 ℃ of the compound DC-4, 12. Open squares show corrected data of dielectric loss with relative dielectric permittivity at different frequencies for planar cell in cooling cycle, solid line is semicircle fit of the data and the broken line is extrapolation for the values of ε(0) and ε'(∞). Where ε(0) is the low frequency limiting value of dielectric permittivity and ε'(∞) is the lowest value of dielectric permittivity corresponding to the soft mode i.e. high frequency limiting value.

alignment (homeotropic), the Cole-Cole fitting of the dielectric data, temperature dependence of relaxation frequency, and magnitude of activations energies in different mesophases suggest that this mode arise due to the rotation of individual molecules about their short axes [22].

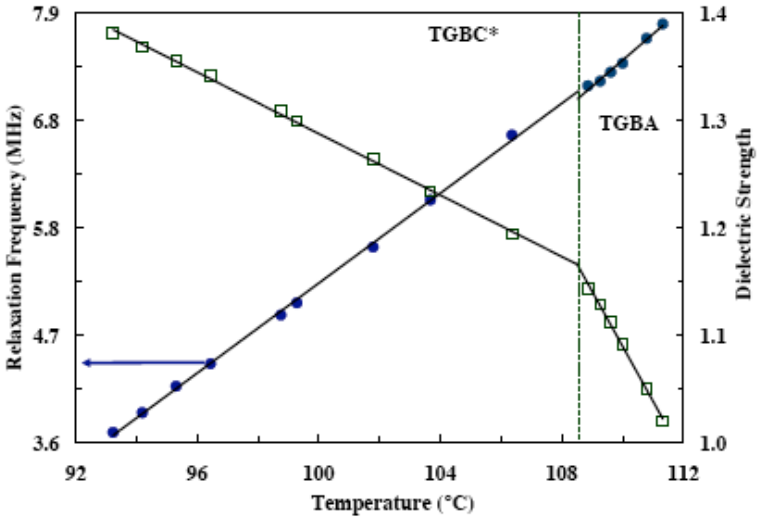

Fig. (6). Temperature dependences of the relaxation frequency, f_r (solid circles) and dielectric strength, $\Delta\varepsilon$ (open squares) of soft mode relaxation in planar anchoring in TGBA and TGBC* phases.

a

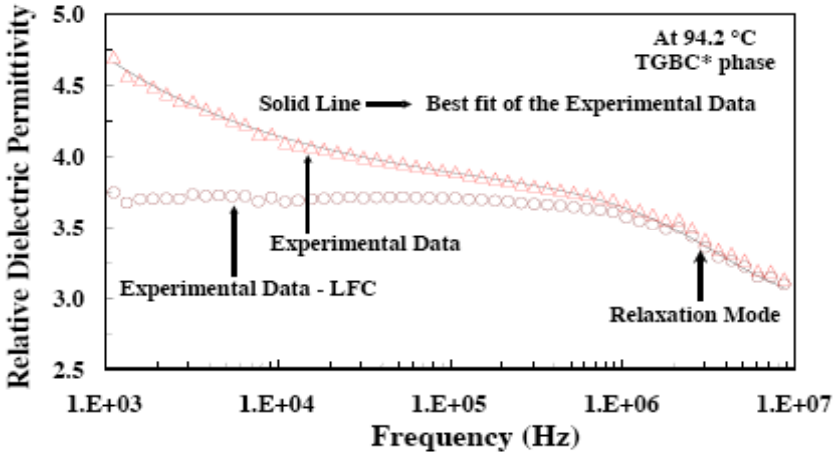

b

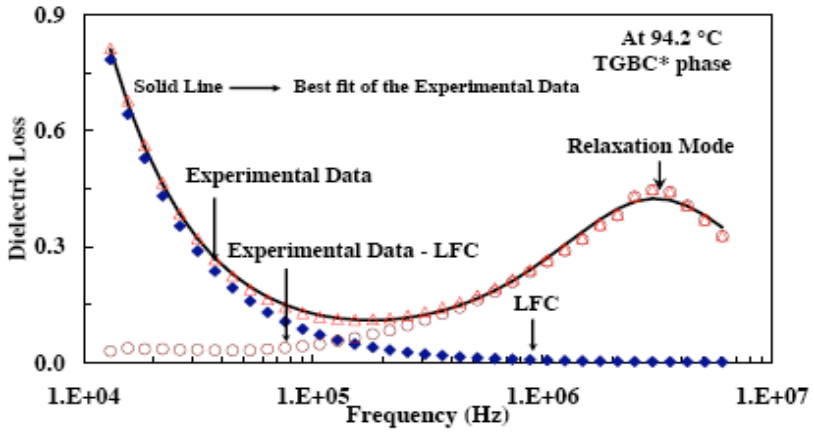

Fig. (7). Frequency dispersion of (**a**) dielectric-permittivity and (**b**) dielectric loss at 94.2 ℃ in the TGBC* phase in homeotropic aligned sample to demonstrate a relaxation mode (on the higher frequency side). The solid line is fit of Cole-Cole formula.

The relaxation frequency of TGBA and TGBC* phases follow Arrhenius behavior as follows:

$$f_r = f_0 \exp\left(-\frac{W_a}{NkT}\right) \quad (7)$$

Where T is the temperature in Kelvin, N is Avogadro number, k (= 1.38x 10^{-23} J-K^{-1}) is the Boltzman constant and W_a is activation energy. We found the activation energy in homeotropic anchoring for TGBA and TGBC* phase is 34.2 kJ/mole and 38.4 kJ/mole respectively (see Fig. (**9a**)), and

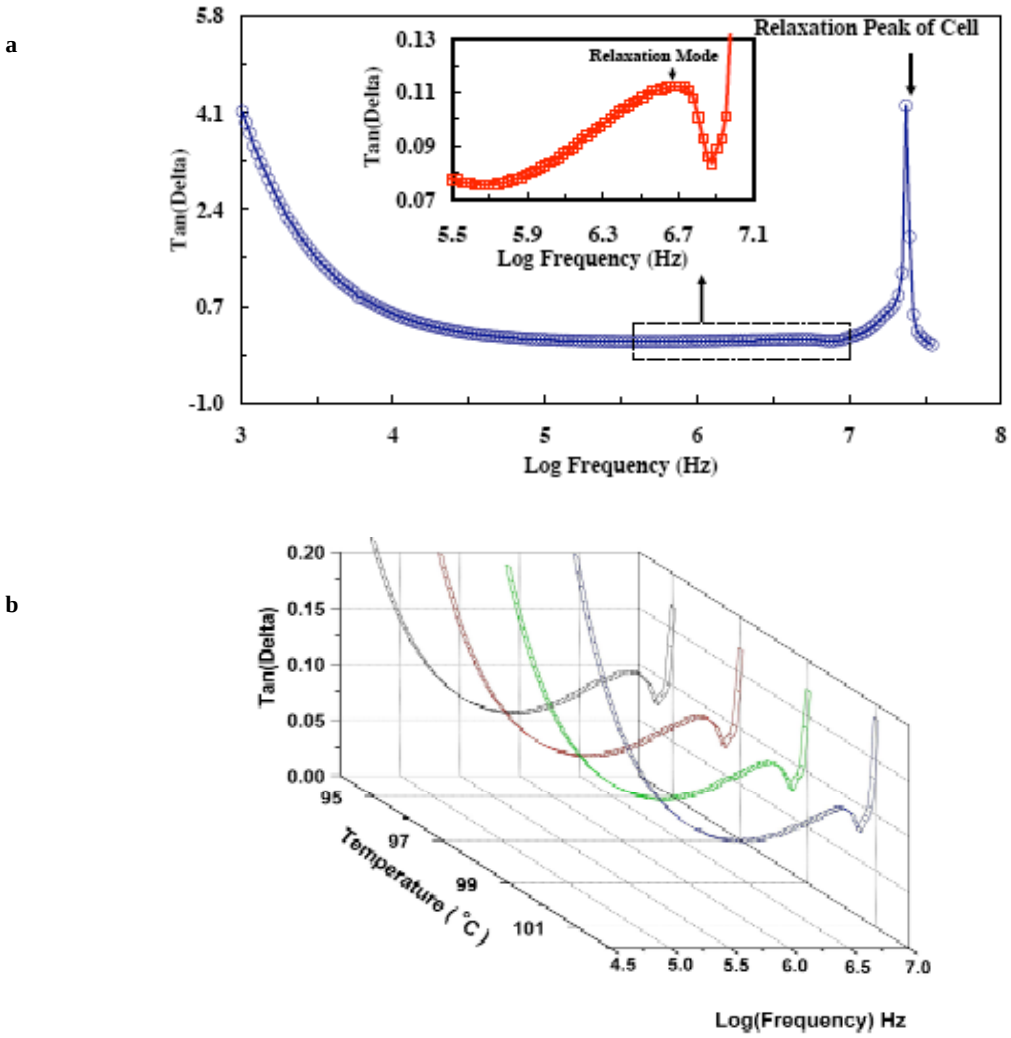

Fig. (8). Frequency dispersion of tan delta demonstrating a relaxation mode in high frequency region for homeotropic aligned sample in the TGBC* phase (a) at 95.0 ℃ shows relaxation mode in inset and (b) A three dimensional plot at temperatures 95.0, 97.0, 99.0 and 101.0 ℃.

for planar anchoring in TGBA and TGBC* phase is 52.4 kJ/mole and 54.0 kJ/mole respectively (see Fig. (**9b**)).

Excluding the immediate vicinity of transition temperatures, the variation of inverse of dielectric strength ($\Delta\varepsilon^{-1}$) with temperature is linear (see Fig. **10**) in both phases (TGBA and TGBC*) for homeotropic and planar alignments. The calculated slopes are:

In homeotropic anchoring:

$(d\Delta\varepsilon^{-1}/dT)_{TGBA} = 0.15\ ℃^{-1}$

$(d\Delta\varepsilon^{-1}/dT)_{TGBC^*} = 0.05\ ℃^{-1}$

In planar anchoring:

$(d\Delta\varepsilon^{-1}/dT)_{TGBA} = 0.040\ ℃^{-1}$

$(d\Delta\varepsilon^{-1}/dT)_{TGBC^*} = 0.008\ ℃^{-1}$

Thus from above one can see that slope of TGBC* phase is less than that of TGBA phase in both planar and homeotropic alignment.

For the comparative study of the rotational viscosity in planar anchoring of molecules for TGBA and TGBC* phases, we use the theoretical expression from Ismaili *et al.*, [21] given as:

$$(\Delta\varepsilon \times f_r)_{TGBA} = \frac{\varepsilon_0 \chi^2 C^2}{2\pi\gamma_{TGBA}} \tag{8a}$$

$$(\Delta\varepsilon \times f_r)_{TGBC^*} = \frac{\varepsilon_0 \chi^2 C^2}{2\pi\gamma_{TGBC^*}} \cos^2(\theta_s) \tag{8b}$$

where γ_{TGBA} and γ_{TGBC^*} are viscosity of relaxation mode of TGBA and TGBC* phases. It is important to point out that $\cos^2(\theta_s)$ is the result of two projections: projection of the applied field say E_x on the smectic planes and projection on the X-direction of the dipoles induced in the smectic planes. This geometric factor is almost equal to unity, since the spontaneous tilt angle is rarely higher than 15° in the TGBC* phase [23].

The plot of $\Delta\varepsilon \times f_r$ versus temperature in Fig. (**11**) shows that the product $\Delta\varepsilon \times f_r$ have higher value in TGBA than in the

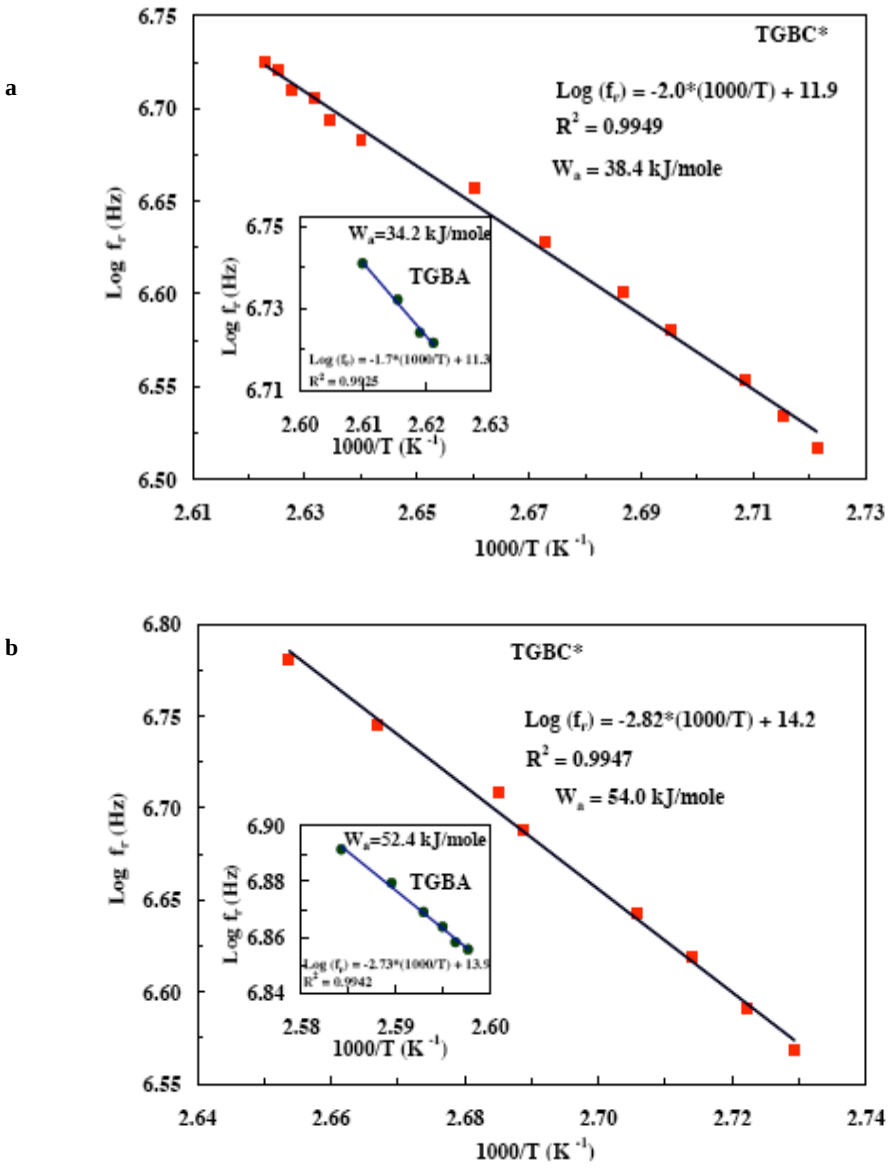

Fig. (9). Arrhenius plot for relaxation frequencies related to the detected relaxation mode in cooling cycle in TGBA and TGBC* phases (**a**) In homeotropic anchoring and (**b**) in planar anchoring of the molecules.

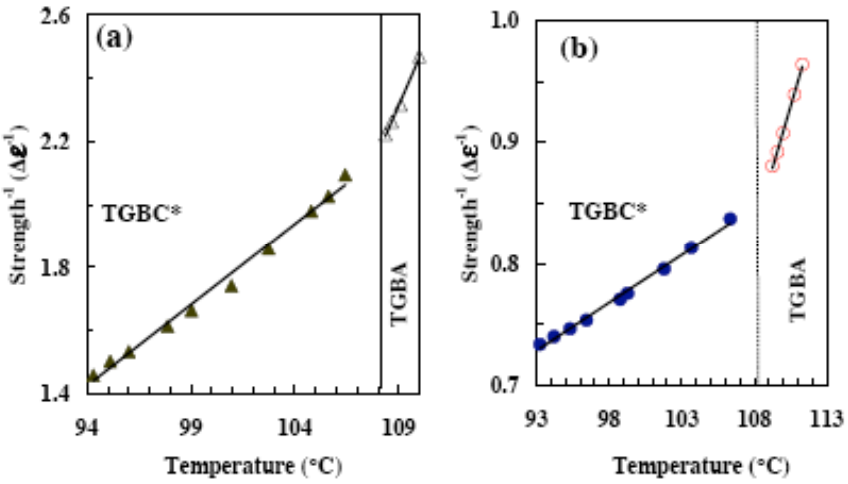

Fig. (10). Variation of inverse of dielectric strength ($\Delta\varepsilon^{-1}$) with temperature. (**a**) In homeotropic anchoring and (**b**) in planar anchoring.

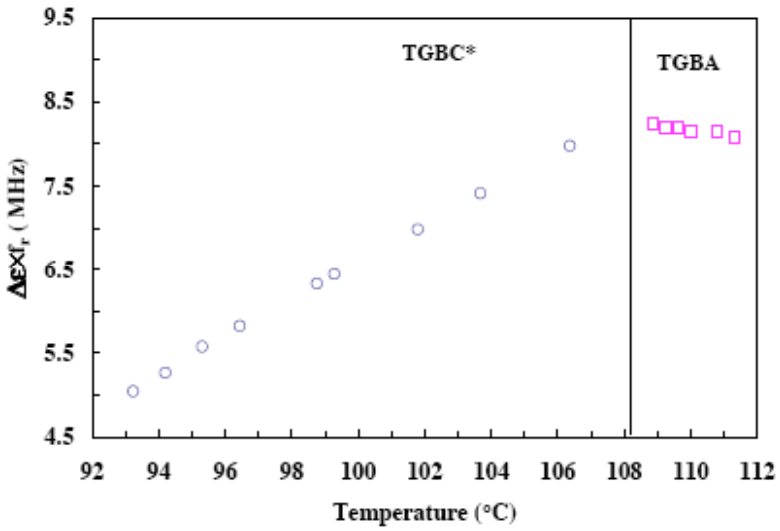

Fig. (11). Variation of $\Delta\varepsilon \times f_r$ with temperature for soft mode like relaxation of planar anchoring of the molecule for all members of the series in TGBA and TGBC* phases.

TGBC* phase, consequently rotational viscosity is expected to be lower in TGBA than in the TGBC* phase. As $\Delta\varepsilon \times f_r$ is approximately constant in TGBA phase, so viscosity is also quasiconstant in this phase [21]. We find that activation energy of TGBA is less whereas relaxation frequency is higher than that of the TGBC* phase. This phenomenon also confirms that viscosity is lower in TGBA than TGBC* phase.

CONCLUSIONS

Present studies suggest that the planar oriented molecules show a soft mode of relaxation due to the tilt fluctuation of molecules in the frequency range of 3-8 MHz for both the TGB (A and C*) phases. A weak mode of relaxation has been detected in homeotropically aligned sample in MHz region for both TGB phases, which is due to the rotation of individual molecules about their short axes. We have found that, with the exception of the near neighborhood of transition temperatures, the variation of inverse of dielectric strength with temperature is linear in both the TGB phases. It has been found that the slopes of TGBC* phase is less than that of the TGBA phase for both the molecular geometries. In planar anchoring of the molecules, it has been found that the product of dielectric strength ($\Delta\varepsilon$) and relaxation frequency (f_r) is higher in TGBA than in TGBC* phase, accordingly the rotational viscosity is expected to lower in the TGBA than in TGBC* phase.

ACKNOWLEDGEMENTS

Authors thank Department of Science and Technology (DST), New Delhi for financial assistance under a Project Grant No. SR/S2/CMP-12/2006. ASP thanks DST for a Senior Research Fellowship under the project. ASP also expresses thanks to CSIR, New Delhi for his present fellowship under its CSIR-SRF scheme. ASP is grateful to Dr. M. B. Pandey for several fruitful discussions on some part of the experimental results.

REFERENCES

[1] Renn SR, Lubensky TC. Abrikosov dislocation lattice in a model of the cholesteric-to-smectic-A transition. Phys Rev A 1988; 38: 2132-47.

[2] Renn SR, Lubensky TC. Existence of a Sm-C grain boundary phase at the chiral NAC point. Mol Cryst Liq Cryst 1991; 209: 349-55.

[3] Renn SR. Multicritical behavior of Abrikosov vortex lattices near the cholesteric-smectic-A-smectic-C* point. Phys Rev A 1992; 45: 953-73.

[4] Dozov I. Melted-Grain-Boundary Phase in Chiral Smectic-C Liquid Crytals near the Triple N*A*C* Point. Phys Rev Lett 1995; 74: 4245-8.

[5] Kamien RD, Lubensky TC. Twisted Line Liquids. J Phys I France 1993; 3: 2131-8.

[6] Petrenko AS, Hird M, Lewis RA, Meier JG, Jones JC, Goodby JW. A twist grain boundary phase with a local antiferroelectric structure. J Phys Condens Matter 2000; 12: 8577-93.

[7] Pansu B, Grelet E, Li MH, Nguyen HT. Hexagonal symmetry for smectic blue phases. Phys Rev E 2000; 62: 658-65.

[8] Goodby JW, Waugh MA, Stein SM, Chin E, Pindak R, Patel JS. Characterization of a new helical smectic liquid crystal. Nature 1989; 337: 449-52.

[9] Goodby JW, Waugh MA, Stein SM, Chin E, Pindak R, Patel JS. A new molecular ordering in helical liquid crystals. J Am Chem Soc 1989: 111: 8119-25.

[10] Dhar R. Twisted-grain-boundary (TGB) phases: Nano structured liquid-crystal analogue of Abrikosov vortex lattices. Phase Transitions 2006; 79: 175-99.

[11] Pandey MB, Dhar R, Wadhawan VK. Phase transitions and recent advances in liquid crystals research. Phase Transitions 2009; 82: 831-49.

[12] Navailles L, Pansu B, Gorre-Talini L, Nguyen HT. Structural Study of a Commensurate TGBA Phase and of a Presumed Chiral Line Liquid Phase. Phys Rev Lett 1998; 81: 4168-71.

[13] Dhar R, Srivastava AK, Agrawal VK. Induced twisted-grain-boundary phases in the binary mixtures of a cholesteric and a nematic compound. Phase Transitions 2003; 76: 959-74.

[14] Yelamaggad CV, Bonde NL, Achalkumar AS, Rao DSS, Prasad SK, Prajapati AK. Frustrated liquid crystals: Synthesis and mesomorphic behavior of unsymmetrical dimers possessing chiral and fluorescent entities. Chem Mater 2007; 19: 2463-72.

[15] Cole KS, Cole RH. Dispersion and absorption in dielectrics. J Chem Phys 1941; 9: 341-51.

[16] Pandey MB, Dhar R, Agrawal VK, Khare RP, Dabrowski R. Low frequency dielectric spectroscopy of two room temperature chiral liquid crystal mixtures. Phase Transitions 2003; 76: 945-58.

[17] Srivastava SL, Dhar R. Characteristic time of ionic conductance and electrode polarization capacitance in some organic liquids by low frequency dielectric spectroscopy. Indian J Pure Appl Phys 1991; 29: 745-51.

[18] Srivastava SL Electrical properties of ferroelectric liquid crystals. Proc Natl Acad Sci India 1993; 63: 311-32.

[19] Dhar R. An impedance model to improve the higher frequency limit of electrical measurements on the capacitor cell made from electrodes of finite resistances. Indian J Pure Appl Phys 2004; 42: 56-61.

[20] Yelamaggad CV, Achalkumar AS, Bonde NL, Prajapati AK. Liquid crystal abrikosov flux phase: the exclusive wide thermal range enantiotropic occurrence. Chem Mater 2006; 18: 1076-78.

[21] Ismaili M, Bougrioua F, Isaert N, Legrand C, Nguyen HT. Dielectric properties of twist grain boundary phases: Influence of the anchoring and the distance between grain boundaries. Phys Rev E 2001; 65: 011701-1-15.

[22] Gupta M, Dhar R, Agrawal VK, Dabrowski R, Tykarska M. Dielectric spectroscopy of a binary mixture of liquid crystals showing wide temperature range twisted grain boundary phase with re-entrant cholesteric phase. Phys Rev E 2005; 72: 021703-1-10.

[23] Navailles L. Ph.D. thesis 1994, University of Bordeaux I, France.

Received: April 07, 2011 Revised: June 13, 2011 Accepted: June 13, 2011